

Intra-tibial injection of human prostate cancer cell line CWR22 elicits osteoblastic response in immunodeficient rats

C. Andresen, C.M. Bagi, S.W. Adams

Pfizer Inc., Global Research and Development, Drug Safety Evaluation, Groton, CT, USA

Abstract

We investigated the utility of CWR22 human prostate cancer cells for modeling human metastatic prostate cancer, specifically their ability to induce bone formation following intra-tibial injections in the nude rat. Prostate cancer is unique in regard to its tropism for bone and ability to induce new bone formation. In contrast to humans, other mammalian species rarely develop prostatic cancer spontaneously upon aging and do not have the propensity for bone metastasis that is the hallmark of cancer malignancy in men. We chose human prostate cancer cell line CWR22 based on its properties, which closely resemble all of the features that characterize the early stages of prostatic cancer in human patients including slow growth rate, hormone dependence/independence and secretion of prostate-specific antigen. When CWR22 cells were injected directly into the proximal tibia of immunodeficient male rats, both osteoblastic and osteolytic features became evident after 4 to 6 weeks, with elevated levels of serum prostate-specific antigen. However, osteosclerosis dominates the skeletal response to tumor burden. Radiological and histological evidence revealed osteosclerotic lesions with trabeculae of newly formed bone lined by active osteoblasts and surrounded by tumor cells. Toward the end of the 7-week study, osteolytic bone lesions become more evident on X-rays. Paraffin and immunohistochemical evaluations revealed mature bone matrix resorption as evidenced by the presence of many tartrate resistant acid phosphatase positive multinucleated osteoclasts. We conclude that the CWR22 human prostate cell line used in an intra-tibial nude rat model provides a useful system to study mechanisms involved in osteoblastic and osteolytic bony metastases. This type of *in vivo* model that closely mimics all major features of metastatic disease in humans may provide a critical tool for drug development efforts focused on developing integrated systemic therapy targeting the tumor in its specific primary or/and metastatic microenvironments. In addition to targeting bone marrow stroma, this strategy will help to overcome classical drug resistance seen at the sites of prostate cancer metastasis to bones.

Keywords: Cancer of the Prostate, Nude Rat, CWR22, Bone Formation, Osteosclerosis, Bone Resorption, Prostate-Specific Antigen, Testosterone

Introduction

Cancer of the prostate (CaP) is unique with regard to its tropism for bone tissue and ability to induce osteoblastic response (osteosclerosis). With the increasing life expectancy of men, CaP has become a major medical problem. Most prostate cancer patients initially respond to anti-androgen therapy due to early testosterone dependence of all prostate cancer. The switch of the cancers cells from hormonal dependence to independence and the resulting relapse in

tumor growth is one of the main clinical problems of prostate cancer¹. Metastatic spread of CaP towards bone signals an incurable disease state and is the main cause of morbidity among prostate cancer patients². In contrast to men, other mammalian species rarely develop prostatic cancer spontaneously upon aging³. This characteristic, in addition to poor growth of available prostate cancer cell lines, are significant barriers to the development of representative animal models of the various stages of human metastatic prostate cancer. In 1991, Petlow et al.⁴ first reported on their efforts to develop a new human prostate tumor xenograft. Properties of the CWR22 tumor cell line include: slow growth rate, hormone dependence/independence and secretion of prostate-specific antigen (PSA), all features that characterize the early stages of prostatic cancer in human patients. In addition, CWR22 is a primary human prostate cancer cell line in which both hormone dependent and hormone independent stages exist.

Corresponding author: Cedo M. Bagi, M.D., Ph.D., Pfizer Inc., Global Research and Development, DSE/CEM, Eastern Point Road 8274-1312, Groton, CT 06340, USA

E-mail: cedo_bagi@groton.pfizer.com

Accepted 6 January 2003



Figures 1A and 1B. Figure 1A depicts X-ray image of intra-tibial injection. Rats were injected extracapsularly through the epiphysis and growth plate ending in tibial metaphysis (arrowhead). Two weeks following intra-tibial injection there is a visible osteosclerotic scar indicating healing process caused by the injection trauma (arrowhead; 1B). No other signs of non-physiological bone formation or resorption were noted on the X-rays and confirmed by paraffin histology as a consequence of injection trauma.

Therefore, this tumor cell line has all the major characteristics of early stage prostate cancer in men⁵. There are scant data available regarding the ability of human prostate cancer cell line CWR22 to grow in the bone microenvironment and characterizing the subsequent development of bone lesions. If indeed this tumor cell line can elicit an osteoblastic bone response with concomitant osteosclerosis, CWR22 cells could be an ideal cell line to study early stages of prostate cancer development and its progression to bones. In this study, we investigated the ability of CWR22 human prostate cancer cells to induce bone formation in nude rats following intra-tibial injection of the tumor cells. We have attempted to describe the osteoblastic and/or osteolytic character of the bone lesions by utilizing different histological and radiological means. Finally, we explored the use of this model to better characterize the initial phase of the prostate cancer metastasis to the skeleton and provide options for exploring novel treatment modalities.

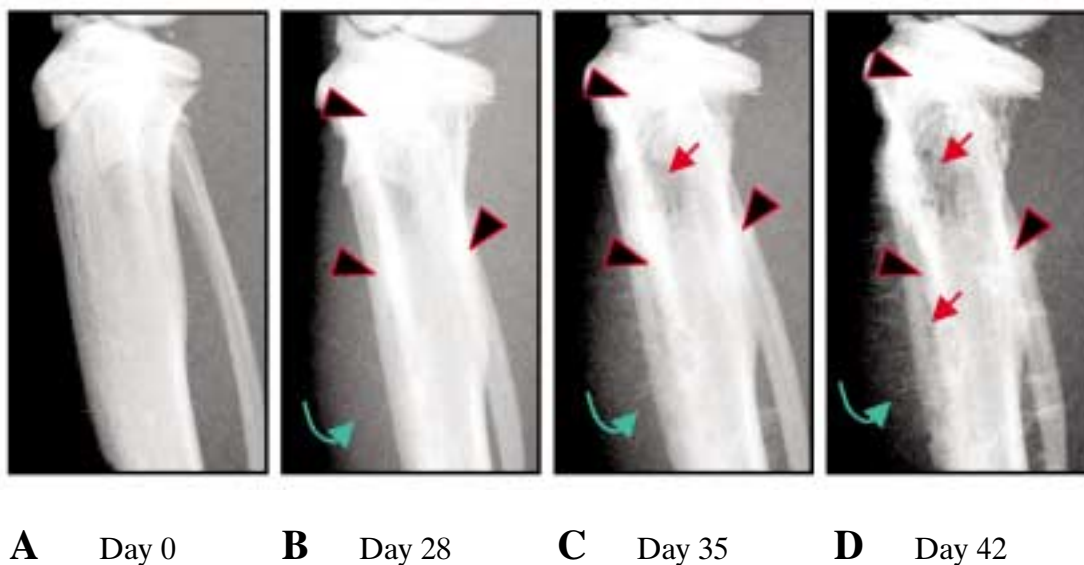
Materials and methods

Cell line and culture conditions. CWR22 human prostate cancer cell line was purchased from the American Type Culture Collection (ATCC, Manassas, VA). The tumor originates from prostate adenocarcinoma and consists of moderately and poorly differentiated carcinoma tissue. The tumor cells were maintained in culture in DMEM-10% fetal bovine serum. Cell line was used at low passage number. The properties of CWR22 tumor cell line; slow growth rate, hormone dependence/independence and secretion of prostate-specific

antigen are comparable with those of prostatic cancer in the patient. CWR22 is a primary human prostate cancer cell line in which both hormone dependent and relapsed versions exist⁴⁻⁷.

Animals. Immunodeficient male homozygous Sprague Dawley rats were purchased from Taconic Farms (Germantown, NY). Rats arrived at 3 months of age and were maintained according to the NIH standards established in the “Guidelines for the Care and Use of Laboratory Animals”. The Internal Animal Care and Use Committee (IACUC) approved experimental protocols. All rats in the study were single housed in polycarbonate microisolator cages lined with autoclaved bedding. Autoclaved reverse osmosis (RO) water and autoclaved standard rat chow were provided ad libitum. Body weights were recorded weekly throughout the course of the study.

Tumor injections. Rats were maintained under isoflurane anesthesia during the tumor injection procedure. The skin surface at the injection site was prepped with betadine scrub followed by alcohol wipe. A 23-gauge needle with one cc syringe was inserted extra-capsularly through the tibial crest, epiphysis and growth plate (Figure 1A). Five million tumor cells in a 0.2 ml volume were injected into the bone marrow space of both tibial metaphysis. The eight rats with X-ray detectable tumors in both tibiae were kept in the study. In addition, four rats were injected in one tibia with the 23-gauge needle while the contralateral tibia served as an intact control to evaluate the effect of injection trauma on bone remodeling. No media alone was injected in this study to test for the non-specific bone response. All rats enrolled in the



Figures 2A-2D. Intra-tibial injection of 105 human CWR22 prostate carcinoma cells elicited osteosclerotic response at 4 weeks after tumor inoculation (black arrowheads). Tumor growth is associated with amorphous, cloud-like calcification in the soft tissue (green arrow) with osteosclerotic specula clearly visible on the outside of the tibial cortex. At week five osteolytic lesions start appearing on the radiographs (red arrows), and by week six osteosclerotic and osteolytic lesions are both clearly visible. Osteosclerotic features dominate radiographic appearance of the CWR22 prostate tumor growth in the bones of nude rats.

study were euthanized six weeks following tumor injections.

Other procedures. Fluorochrome bone marker calcein (Sigma, St. Louis, MO) was given as i.p. and s.c. injections (12.5 mg/kg each) 3 days prior to euthanasia. Testosterone (Sigma), (3 mg/kg) was given twice per week by s.c. injection as a suspension prepared at 3 mg/ml in sesame oil. Testosterone concentration in serum was measured twice, at the beginning of the study before tumor inoculation and at the end of the study. Testosterone was administered to all animals to minimize variations in tumor growth between individual rats since serum testosterone substantially varied between rats before tumor inoculation.

Blood collection. Blood was collected weekly by retro-orbital bleed for hematology and serum chemistry measurements. Animals were lightly anesthetized during the bleed procedure with CO₂/O₂. Hematology parameters were analyzed on a Bayer Advia 120. Chemistry endpoints were analyzed using Hitachi 917 auto-analyzer. Terminal blood was taken under CO₂ anesthesia by cardiac puncture. Serum levels of prostate-specific antigen and testosterone were measured using Clinigamma analyzer by RIA.

Urine. Urine was collected during a five-hour fasting period, one day prior to termination using a metabolism cage. Samples were analyzed for creatinine, phosphorus and calcium using auto-analyzer Hitachi 917.

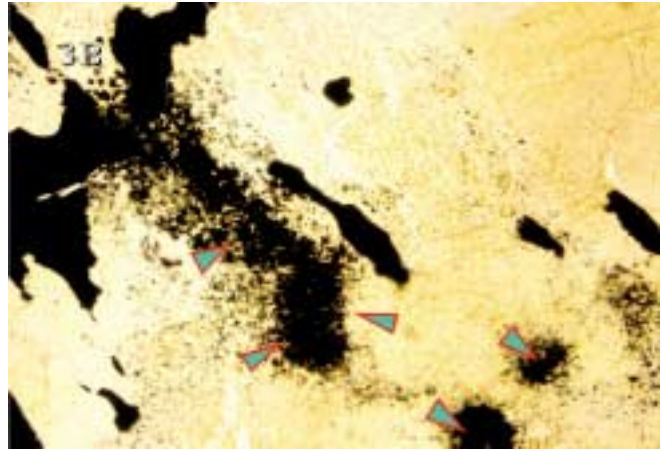
Radiography. X-rays were taken of each of the hind limbs once per week using a Faxitron® (Faxitron X-ray Corporation, Wheeling, IL) digital capture X-ray at kv 26, magnification 1.5 and 2-second exposure. Rats were anesthetized for the X-

ray procedure with isoflurane. No attempts were made to quantify tumor growth from the X-rays due to loss of bone anatomy with the progression of tumor growth. However, tumor progression was monitored weekly by comparing new X-ray images with the ones obtained the previous week.

Histology. Decalcified bone. At the end of the study the right rat tibias were excised and placed in 4°C, 10% neutral buffered formalin (Decal. Congers, NY) for three days to allow for fixation. Tibias were then washed with cold running tap water for one hour then placed in 5% EDTA at 4°C for decalcification, and paraffin processed. Sections were cut at 5 µm, stained with hematoxylin and eosin (H&E) and osteoclasts were stained with Tartrate-resistant Acid Phosphatase (TRAP) using a Leukocyte Acid Phosphatase Kit #387-A (Sigma Diagnostics, Inc., St. Louis, MO). Cell number and morphology were evaluated in the proximal tibial metaphyses.

Undecalcified bone. The left tibias were fixed in neutral buffered formalin for 48 hours, dehydrated with a series of graded ethanols and embedded in methyl-methacrylate. Longitudinal sections of the proximal half of the tibias were cut at 4 and 10 µm in thickness and analyzed under UV light for the presence of fluorochrome label (calcein) at the areas affected by the prostate cancer.

Statistical Analysis. Statistical analysis of the data was performed by a nonparametric test (Wilcoxon's test) or Student's t-test (when indicated). Differences were considered to be statistically significant when a p value of <0.05 was found.



Figures 3A and 3B. Examples of osteosclerotic, fully mineralized, newly formed bone surrounded by the tumor cells. Figure 3A depicts new "rod-like" bone formation (green arrowheads) perpendicular to old cortex. Figure 3B depicts example of "spot-like" calcification (green arrowheads) inside tibial metaphysis clearly distinguishable from old trabeculae. Bone marrow is almost entirely replaced with tumor cells. The image was obtained from von Kossa stained section. Magnification x10.

Results

The number of animals developing tumors following inoculation of tumor cells was high and at the end of the study tumor mass was detectable in both tibiae of each of the eight rats enrolled in the study. Signs of local invasion were seen in several rats with tumor penetrating bone cortex and growing locally into soft tissue next to the bone. As expected, distant metastases in visceral organs or bones other than tibia were not found at necropsy.

Body weight. During the course of the study all rats were eating well and on average each animal gained approximately 10% of their initial body weight.

Serum chemistry. Serum markers including total alkaline phosphatase, calcium, phosphorus, and creatinine were measured weekly. No statistically significant difference was seen in serum chemistry markers between day 0 (before tumor inoculation) and day 42 (end of the study).

Serum testosterone. Serum testosterone measured before tumor inoculation substantially varied between individual animals (158 to 523 ng/dL). Serum testosterone measured from blood samples drawn on the final day of the study prior to euthanasia was within narrow limits in all rats with a mean value of 205.83 ± 12.3 ng/dL.

Prostate-specific antigen. Serum PSA was measured from blood samples drawn on the final day of the study prior to euthanasia. PSA was not detectable in controls (assay limit 0.01 ng/mL) and was 0.184 ± 0.091 ng/mL in rats administered the CWR22 cell line. Qualitative analysis of Faxitron tumor images showed a trend towards higher PSA levels in rats with the greatest tumor burden (data not shown).

Urine chemistry. At the end of the study calcium, phosphorus and creatinine in urine were all within the normal physiological range. The two rats with the highest tumor

burden (and highest PSA values) showed the highest calcium/phosphorus ratios 1.24 and 0.84 respectively, compared to 0.39, which was the average for the rest of the group.

X-ray analysis. The sites of intra-tibial injections in all rats were visible on the X-rays at week one and two. Rats that received no tumor cells or media showed signs of bone healing seen as a mild sclerosis at the site of injection probably due to callus formation (week 2, Figure 1B). Radiographic data revealed the appearance of osteosclerotic bone lesions 3 to 4 weeks following intra-tibial injection of CWR22 human prostate tumor. Also, the growth of the tumor is radiologically evident from the formation of amorphous, cloud-like calcification in the soft tissue. The intensity of osteosclerosis gradually increased as time passed after inoculation of the tumor cells (Figures 2A to 2D). Approximately 4 to 5 weeks post-inoculation osteolytic bone lesions became visible. Endosteal scalloping with development of bone transparencies that gradually increased in size was evident by week 5 (Figures 2C and 2D). All experimental animals showed a certain degree of radiologically evident osteosclerosis and osteolysis in both tibiae, suggesting tumor progression from purely osteoblastic to a mixed phenotype. Similar changes in men are the hallmark of metastatic prostate cancer.

Histology. Undecalcified bones bearing tumors showed a high degree of mineralization at areas with osteosclerotic changes when stained by the von Kossa method for mineral (Figures 3A and 3B). Newly formed bone (also visible on the X-rays) appeared as a calcified, spindle-shaped trabeculae perpendicular to the tibial cortex (3A), or as a "spot-like" intraosseal sclerosis (3B) on the von Kossa stained slides. Both osteosclerotic formations are clearly distinguishable from the old bone matrix. The fluorochrome labeling of the osteosclerotic bone showed intensive fluorescence under the UV light indicating rapid collagen ossification (Figures 4A and 4B).

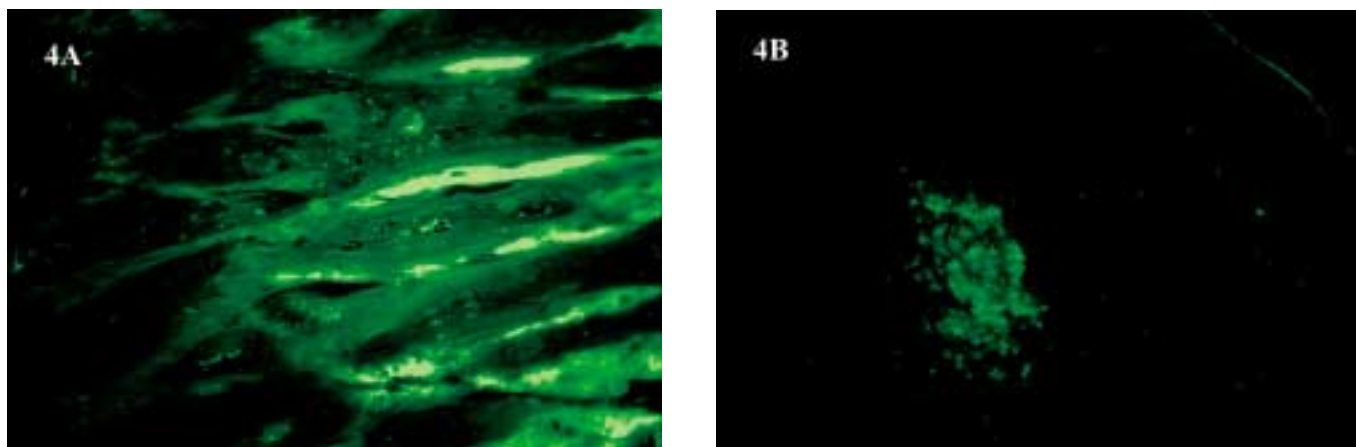


Figure 4A and 4B. Typical detail illustrating intensive fluorochrome labeling of newly formed "spindle-like" bone (4A) such as one shown in Figure 3A, and "spot-like" calcification (4B) such as one shown in Figure 2B. Calcein was injected 3 days before the necropsy. Undecalcified, unstained 4 μ m thick longitudinal section of the proximal tibia bearing CWR22 tumor. Microradiograph was taken under UV light. Magnification x10.

Paraffin histology and TRAP immunohistology. Paraffin histology revealed a large tumor mass within the tibias of rats injected with CWR22 cells. The bone marrow has been largely replaced with the tumor cells. The nests of the tumor cells are composed of small and medium-sized principal cells that vary in shape and appear hyperchromatic (Figure 5A). Old bone matrix is clearly distinguishable from the newly formed bone. Numerous multinucleated TRAP+ cells (osteoclasts) are clearly visible covering the old bone matrix (Figure 5B) and indicate extensive bone resorption as judged by the cell size, number of nuclei and scalloped bone surfaces below the cells. Surfaces of the newly formed bone are covered with osteoblasts indicating extensive bone formation with very few and rather small osteoclasts.

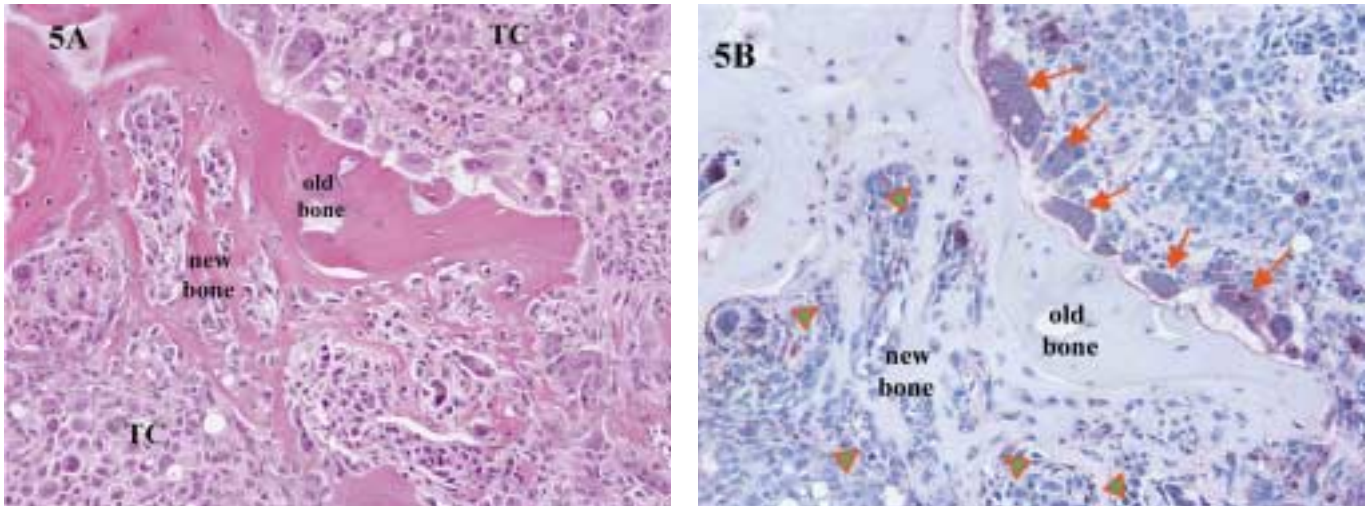
Discussion

Historically, for *in vivo* models, human tumors have been implanted subcutaneously⁸. The incidence of subcutaneous primary malignant tumors or metastases is extremely rare in all mammals. The subcutaneous microenvironment is very different from the tissue of origin of the primary tumors and sites of metastasis such as lungs, liver and bones. Human tumor cells subcutaneously implanted in immunodeficient rodents lose their innate ability to invade the circulatory system and cause distant metastases. In addition, it has been documented that radical differences exist in drug response of tumors in the orthotopically or metastatic tissue sites compared to tumors growing subcutaneously^{9,10}.

The phenomenon of prostate cancer metastasis to bone has been difficult to mimic in animal models. In syngeneic animal prostate cancer models such as the Dunning rat model¹⁰ and the transgenic mouse model¹¹ lymph node and pulmonary metastases are common, but the occurrence of bone metastases from a primary tumor site are rare. It is

equally difficult to mimic clinical patterns of bony metastases by using immunodeficient rodent models of human prostate cancers. Various experimental variations utilizing mice and rats¹² have been used in the past to address pathophysiology of bone metastasis including co-injections of tumor cells with bone stromal cells¹³ or with human bone tissue¹⁴, intracardiac injections¹⁵, orthotopic injection of prostate tumor cells to bone¹⁶, or brief occlusion of the vena cava during intravenous injections of tumor cells¹⁷. Despite the initial difficulties regarding development of an animal model¹⁸, the molecular mechanisms underlying osteolytic bone metastases are well described¹⁹⁻²². As a consequence of improved understanding of the role that the bone environment plays in disease progression, therapeutic modalities targeting bone stromal cells have proven to be a very efficacious way of dealing with lytic bone metastases in breast and prostate cancer patients^{23,24}. Our experience over the last decade by using different osteolytic breast and prostate tumor cell lines in different experimental setups provided data that closely predicted the clinical outcome of antiresorptive therapies such as the new generation of nitrogen-containing bisphosphonates²⁴⁻²⁷.

Prostate-specific antigen (PSA) is expressed in more than 99% of all prostate cancers and is a very reliable marker for monitoring the disease and response to therapy²⁸. All prostate cancers in humans are androgen dependent in their early stage. Recent improvements in the diagnosis and screening of prostate cancer have identified an increasing number of patients with lesions confined to the prostate, even though results from bone biopsies show that between 35 and 75 percent of those patients tested positive for tumor cells. Because of unpredictable biological potential and the clinical course that disease may take, bone metastases represent a serious threat even though disease has been diagnosed early. Since the majority of prostate cancer patients experi-



Figures 5A and 5B. Intra-tibial injection of 10^5 human CWR22 prostate carcinoma cells elicited osteosclerotic and osteolytic response. Figure 5A (H&E) depicts old bone matrix surrounded by the tumor cells, and new bone matrix formed as a consequence of tumor. Figure 5B (TRAP) is showing the same bone detail as the one seen in Figure 5A. The numerous multicellular osteoclasts (TRAP⁺; red arrows) can be seen engulfing the old bone matrix. At the same figure, osteoblasts (green arrowheads) are depositing a new bone matrix.

ence osteoblastic type of bone metastases, identification of a human prostate cancer cell line that will reproducibly induce osteosclerotic bone changes will be highly desirable. In the past, because of non-availability of human prostate tumor cell lines with osteoblastic potential, several studies have been performed on rat models of osteoblastic metastasis. Pollard and Luckert²⁹ developed a model using Lobund-Wistar rats that develop spontaneous adenocarcinoma, but limitations include long incubation periods before tumor induction (a year or longer) and low tumor incidence (10%). Also, these tumors lack the testosterone receptor and do not cause spontaneous bone metastases and therefore are not suitable for drug discovery or drug validation. Finally, prostate cancer can be induced in rodents by either testosterone alone, or in combination with estrogen within a year, but the limitations mentioned earlier are hard to overcome if such models are to be used to develop anticancer therapies.

Currently, there are few established prostate cancer cell lines suitable for study both in tissue culture and in clinically relevant animal model systems. The properties of the CWR22 tumor cell line; slow growth rate, hormone dependence/independence and secretion of PSA are comparable with those of prostatic cancer in man. The CWR22 is a primary human prostate cancer cell line of which both hormone dependent and relapsed versions exist^{4,8}. Our results show that this cell line has yet another crucial property of the human prostate cancer, that is to induce osteoblastic bone response when injected in the proximal tibial metaphysis of the nude rat. Osteosclerotic lesions seen on X-ray closely mimic those seen in the prostate cancer patients with bone metastases. Bone lesions are characterized by increased osteoblastic activity associated with a fibrous stroma. The normal trabecular and cortical architecture is overlaid by

new bone deposited on quiescent surfaces. The newly formed bone appears to be fully mineralized, as judged by X-ray appearance, von Kossa staining for mineral and by fluorochrome labeling. At the moment it is unclear whether the newly formed bone has any mechanical purpose in the skeleton. Similar sclerotic structures in men are the main cause of neurological symptoms and bone pain due to nerve compression. The trabeculae of the newly formed bone were lined by active osteoblasts and surrounded by the tumor cells. In attempts to explain the predominantly osteosclerotic nature of CaP many osteoblast stimulating factors produced by cancer cells have been described including peptides with selective mitogenic activity for osteoblasts, these include: urokinase-type plasminogen activator, TGF- β , IGF-I, FGF, BMP-6 and ET-1³⁰⁻³³.

Even though it has been proposed that tumor cells are capable of eroding bone directly by producing proteolytic enzymes, much more important is the indirect action of cancer cells on bone resorption through the osteoclasts. Evidently CWR22 tumor cells are capable of inducing bone resorption that is the late event in prostate cancer patients with bone metastases. It is not rare to see osteosclerotic lesions next to the areas of bone resorption similar to the one depicted in Figure 2D. The higher calcium/phosphorus ratio detected in the urine of two rats with the highest tumor burden in this study may indicate more vigorous development of osteolytic metastases with tumor progression and consequent increase in renal calcium excretion. In addition there is a strong correlation between the tumor burden in rats, PSA levels in serum and urinary calcium. Urinary pyridinium excretion is augmented in patients with active disease, and indeed, bone resorption markers correlate well with the extent of bone metastases^{34,35}. Human prostate can-

cer cells express Receptor Activator of NF-Kappa B ligand (RANKL) and osteoprotegerin (OPG) particularly when they metastasize to bones, which could further influence vigorous bone remodeling³⁶ and improve survival of hormone-resistant prostate cancer cells³⁷. Numerous TRAP+ osteoclasts seen at the scalloped bone surfaces (Figure 5) testify for the vigorous bone resorption promoting the growth of the tumor by release of the numerous growth factors stored in the bone matrix^{38,39}. It is also worth mentioning that prostate tumors like many other tumors are capable of producing parathyroid hormone related peptide (PTHrP), which contains proteins involved in the regulation of both bone resorption and bone formation^{40,41}. The presence of PTHrP is associated with all lytic tumors and is believed to be a major cause of hypercalcemia of malignancy⁴².

Our data suggest that the CWR22 cell line when used in a combination of several orthotopic models (including one described here) can provide data valuable to further the understanding of the biology of metastatic prostate cancer. Without suitable orthotopic animal models, development and testing of novel therapies aimed to target not only the tumor cells, but also the stroma of the bone marrow will be simply impossible. Finding an efficacious single or combination therapy that is potent enough to eliminate or reduce the tumor burden in the skeleton and slow disease progression is much needed since all current therapies fail once bone metastases develop. The CWR22 human prostate cell line used in the intra-tibial nude rat model provides a useful system to study mechanisms involved in bony metastases of androgen-dependent/independent, PSA positive human prostate cancer with ability to form osteosclerotic lesions.

Acknowledgments

We would like to thank Dr. Jitesh Jani and Earl Emerson for kindly providing tumor cells for this study, Dr. Hua Zhu Ke and Hong Qi for preparing undecalcified bone sections, Kim Kowsz for histopathology support, the DSE Clinical Pathology lab for serum and urine analysis and Jamie Whitman-Sherman for assistance with retroorbital bleeding procedures. We are also thankful to Steve Victoria for his excellent care of the animals and his technical assistance and support throughout the study.

References

1. Newling DW. The geography of prostate cancer and its treatment in Europe. *Cancer Surv* 1995; 23:289-296.
2. Peterson MC. Bone metastases in breast cancer, prostate cancer and myeloma. *Bone* 1987; 8(Suppl.):17-22.
3. Bosland MC. Animal models for the study of prostate carcinogenesis. *J Cell Biochem* 1992; 16(Suppl.):89-98.
4. Pretlow TP, Giaconia JM, Edgehouse NL, Schwartz S, Kung HJ, de Vere White RW, Gumerlock PH, Resnick MI, Amini SB, Pretlow TG. Transplantation of human prostatic carcinoma into nude mice in matrigel. *Cancer Res* 1991; 51:3814-3817.
5. Nagabhushan M, Miller CM, Pretlow TP, Giaconia JM, Edgehouse NL, Schwartz S, Kung HJ, de Vere White RW, Gumerlock PH, Resnick MI, Amini SB, Pretlow TG. CWR22: The first human prostate cancer xenograft with strongly androgen-dependent and relapsed strains both *in vivo* and in soft agar. *Cancer Res* 1996; 56:3042-3046.
6. Kochera M, Depinet TW, Pretlow TP, Giaconia JM, Edgehouse NL, Pretlow TG, Schwartz S. Molecular cytogenetic studies of a serially transplanted primary prostatic carcinoma xenograft (CWR22) and four relapsed tumors. *Prostate* 1999; 41:7-11.
7. Pretlow TG, Wolman SR, Micale MA, Pelley RJ, Kursh ED, Resnick MI, Bodner DR, Jacobberger JW, Delmoro CM, Giaconia JM, Pretlow TP. Xenografts of primary human prostatic carcinoma. *J Natl Cancer Inst* 1993; 85:394-398.
8. Willmans C, Fan D, O'Brian CA, Bucana CD, Fidler IJ. Orthotopic and ectopic organ environments differentially influence the sensitivity of murine colon carcinoma cells to doxorubicin and 5-fluorouracil. *Int J Cancer* 1992; 52:98-104.
9. Fidler IJ. Critical factors in the biology of human cancer metastasis: Twenty-eighth GHA Clowes memorial award lecture. *Cancer Res* 1990; 50:6130-6138.
10. Kuo T-H, Kubota T, Watanabe M, Furukawa T, Kase S, Tanino H, Nishibori H, Saikawa Y, Ishibiki K, Kitajama M, Hoffman RM. Site-specific chemosensitivity of human small-cell lung carcinoma growing orthotopically compared to subcutaneously in SCID mice: The importance of orthotopic models to obtain relevant drug evaluation data. *Anticancer Res* 1993; 13:627-630.
11. Isaacs JT, Isaacs WB, Feitz WFJ, Scheres J. Establishment and characterization of seven Dunning rat prostatic cancer cell lines and their use in developing methods for predicting metastatic abilities of prostatic cancers. *Prostate* 1986; 9:961-981.
12. Zhou HE, Li C-L, Chung LWK. Establishment of human prostate carcinoma skeletal metastasis models. *Cancer* 2000; 88(Suppl.12):2995-2301.
13. Gingrich JR, Barrios RJ, Morton RA, Boyce BF, DeMayo FJ, Finegold MJ, Angelopoulou R, Rosen JM, Greenberg NM. Metastatic prostate cancer in a transgenic mouse. *Cancer Res* 1996; 56:4096-4102.
14. Nemeth JA, Harb JF, Barroso U-Jr, He Z, Grignon DJ, Cher ML. Severe combined immunodeficient-hu model of human prostate cancer metastasis to human bone. *Cancer Res* 1999; 59:1987-1993.
15. Thalmann HN, Anezinis PE, Chang SM, Zhou HE, Kim EE, Hopwood VL, Pathak S, von Eschenbach EA, Chung LWK. Androgen-independent cancer progression and bone metastasis in the LNCaP model of human prostate cancer. *Cancer Res* 1994; 54:2577-2581.
16. Yoneda T. Cellular and molecular mechanisms of breast and prostate cancer metastasis to bone. *Eur J Cancer* 1998; 34:240-245.
17. Sato N, Gleave ME, Bruchovsky N, Rennie PS, Beraldi E, Sullivan LDA. A metastatic and androgen-sensitive human prostate cancer model using intraprostatic inoculation of LNCaP cells in SCID mice. *Cancer Res* 1997; 57:1584-1589.
18. Shevrin DH, Kukreja SC, Ghosh L, Lad TE. Development of skeletal metastasis by human prostate cancer in atymic nude mice. *Clin Exp Metastasis* 1988; 6:401-409.
19. Galasko CSA. Mechanism of lytic and blastic metastatic disease of bone. *Clin Orthop* 1982; 169:20-27.
20. Bundred NJ, Ratcliffe WA, Walker RA, Coley S, Morrison JM, Ratcliffe JG. Parathyroid hormone related protein and hypercalcemia in breast cancer. *BMJ* 1991; 303:1506-1509.
21. Guise TA, Yin JJ, Taylor SD, Kumagai Y, Dallas M, Boyce

- BF, Yoneda T, Mundy GR. Evidence for a causal role of parathyroid hormone related protein in breast cancer-mediated osteolysis. *J Clin Invest* 1996; 98:1544-1549.
22. Guise TA, Mundy GR. Cancer and bone. *Endocr Rev* 1998; 19:18-54.
 23. Arguello F, Baggs RB, Frantz CN. A murine model of experimental metastasis to bone and bone marrow. *Cancer Res* 1988; 48:6876-6881.
 24. Lipton A, Theriault RL, Hortobagyi GN, Simeone J, Knight RD, Mellars K, Reitsma DJ, Heffernan M, Seaman JJ. Pamidronate prevents skeletal complications and is effective palliative treatment in women with breast cancer and osteolytic bone metastases: long-term follow-up of two randomized, placebo controlled trials. *Cancer* 2000; 88:1082-1090.
 25. Papapoulos SE, Hamdy NAT, van der Pluijm G. Bisphosphonates in the management of prostate carcinoma metastatic to the skeleton. *Cancer* 2000; 88(Suppl.12):3047-3053.
 26. Boissier S, Magneto S, Frappart L, Cuzin B, Ebetino FH, Delmas PD, Clezardin P. Bisphosphonates inhibit prostate and breast carcinoma cell adhesion to unmineralized and mineralized bone extracellular matrices. *Cancer Res* 1997; 57:3890-3894.
 27. Russell RG, Rogers MJ, Frith JC, Luckman SP, Coxon FP, Benford HL, Croucher PI, Shipman C, Fleisch HA. The pharmacology of bisphosphonates and new insights into their mechanisms of action. *J Bone Min Res* 1999; 14(Suppl.2):56-65.
 28. Stenman U-H, Leinonen J, Zhang W-M, Finne P. Prostate-specific antigen. *Semin Cancer Biol* 1999; 9:83-93.
 29. Pollard M, Luckert PH. Production of autochthonous prostate cancer in Lobund-Wistar rats by treatment with N-nitroso-N-methylurea and testosterone. *J Natl Cancer Inst* 1986; 77:583-587.
 30. Rabbani SA, Mazar AP, Bernier SM, Haq M, Bolivar I, Henkin J. Structural requirements for the growth factor activity of the amino-terminal domain of urokinase. *J Biol Chem* 1992; 267:1-4.
 31. Koutsilieris M, Frenette G, Lazure C, Lehoux JG, Govindan MV, Polychronakos C. Urokinase-type plasminogen activator: a paracrine factor regulating the bioavailability of IGFs in PA-III cell-induced osteoblastic metastases. *Anticancer Res* 1993; 13:481-486.
 32. Autzen P, Robson CN, Bjartell A, Malcolm AJ, Johnson MI, Neal DE. Bone morphogenetic protein 6 in skeletal metastases from prostate cancer and other common malignancies. *Br J Cancer* 1998; 78:1219-1223.
 33. Orr FW, Lee J, Duivenvoorden WCM, Singh G. Pathophysiologic interactions in skeletal metastasis. *Cancer* 2000; 88(Suppl.12):2912-2918.
 34. Urwin GH, Percival RC, Harris S, Beneton MN, Williams JL, Kanis JA. Generalised increase in bone resorption in carcinoma of the prostate. *Eur J Urol* 1985; 57:721-723.
 35. Percival RC, Urwin GH, Harris S, Watson ME, McCloskey M, Kanis JA. Biochemical and histological evidence that carcinoma of the prostate is associated with increased bone resorption. *Eur J Surg Oncol* 1987; 13:41-49.
 36. Brown JM, Corey E, Lee ZD, True LD, Yun TJ, Tondravi M, Vessella RL. Osteoprotegerin and RANK ligand expression in prostate cancer. *Urology* 2001; 57:611-616.
 37. Holen I, Croucher PI, Hamdy FC, Eaton CL. Osteoprotegerin (OPG) is a survival factor for human prostate cancer cells. *Cancer Res* 2002; 62:1619-1623.
 38. Ware JL. Growth factors and their receptors as determinants in the proliferation and metastasis of human prostate cancer. *Cancer Metastasis Rev* 1993; 12:287-2301.
 39. Pfeilschifter J, Mundy GR. Modulation of transforming growth factor beta activity in bone cultures by osteotropic hormones. *Proc Natl Acad Sci USA* 1987; 84:2024-2028.
 40. Guise TA, Yin JJ, Taylor SD, Kumagai Y, Dallas M, Boyce BF, Yoneda T, Mundy GR. Evidence for a causal role of parathyroid hormone-related protein in the pathogenesis of human breast cancer-mediated osteolysis. *J Clin Invest* 1996; 98:1544-1549.
 41. Blomme EAG, Dougherty KM, Pienta KJ, Capen CC, Rosol TJ, McCauley LK. Skeletal metastasis of prostate adenocarcinoma in rats: Morphometric analysis and role of parathyroid hormone related protein. *Prostate* 1999; 39:187-197.
 42. Martin TJ, Mundy GR. Hypercalcemia of malignancy. In: Martin TJ, Raisz LG (eds) *Clinical endocrinology of calcium metabolism*. Dekker, New York; 1987:171-199.